NASA TECHNICAL NOTE

EFFECT OF MINOR REACTIVE METAL ADDITIONS ON FRACTURE TOUGHNESS OF IRON - 12-PERCENT-NICKEL ALLOY AT -196° AND 25° C

Walter R. Witzke and Joseph R. Stephens

Lewis Research Center

Cleveland, Ohio 44135

NATIONAL AERONAUTICS AND SPACE ADMINISTRATION • WASHINGTON, D. C. • MAY 1976

1. Report No. NASA TN D-8232	2. Government Accession No.	3. Recipient's Catalog No.
4. Title and Subtitle EFFECT OF MINOR REACTIVE METAL ADDITIONS ON FRACTURE TOUGHNESS OF IRON - 12-PERCENT- NICKEL ALLOY AT -196° AND 25° C		5. Report Date May 1976
		6. Performing Organization Code
7. Author(s) Walter R. Witzke and Joseph R. Stephens		8. Performing Organization Report No. E-8555
9. Performing Organization Name and Address Lewis Research Center National Aeronautics and Space Administration Cleveland, Ohio 44135		10. Work Unit No. 506-16
		11. Contract or Grant No.
12. Sponsoring Agency Name and Address National Aeronautics and Space Administration Washington, D. C. 20546		13. Type of Report and Period Covered Technical Note
		14. Sponsoring Agency Code

15. Supplementary Notes

16. Abstract

The slow bend precracked Charpy fracture toughness and tensile behavior of arc-melted and hot-rolled Fe-12Ni alloys containing up to 4 atomic percent reactive metal additions were determined at -196° and 25° C after water quenching from three annealing temperatures. The fracture toughness of Fe-12Ni at -196° C was improved by small amounts of Al, Ce, Hf, La, Nb, Ta, Ti, V, Y, and Zr, but not by Si. Cryogenic toughness was improved up to 7.5 times that of binary Fe-12Ni and varied with the reactive metal, its concentration, and the annealing temperature.

17. Key Words (Suggested by Author(s)) Iron-nickel alloys; Reactive metals additions; Fracture toughness; Cryogenic; Liquid nitrogen; Yield strength; Annealing effects	18. Distribution Statement Unclassified - unlimited STAR Category 26 (rev)		
19. Security Classif. (of this report) Unclassified	20. Security Classif. (of this page) Unclassified	21. No. of Pages 38	22. Price* $4.00

* For sale by the National Technical Information Service, Springfield, Virginia 22161

CONTENTS

EFFECT OF MINOR REACTIVE METAL ADDITIONS ON FRACTURE TOUGHNESS

OF IRON - 12-PERCENT-NICKEL ALLOY AT -196° AND 25° C

by Walter R. Witzke and Joseph R. Stephens

Lewis Research Center

SUMMARY

Iron - 12-atomic-percent-nickel (Fe-12Ni) alloys containing up to 4 atomic percent reactive metal additions were melted and fabricated into sheet. The hot-rolled alloys were annealed at three temperatures, representing zero, partial, or complete transformation to austenite, and then water quenched. Slow bend precracked Charpy fracture toughness and tensile behavior were determined at -196° and 25° C. Alloy microstructures were examined and second-phase particles were extracted and identified.

Toughness varied with the reactive metal, its concentration, and the annealing temperature. The fracture toughness of Fe-12Ni at -196° C was improved by small additions of aluminum (Al), cerium (mischmetal), hafnium, lanthanum, niobium (Nb), tantalum, titanium, vanadium, yttrium, and zirconium, but not by silicon. Toughness values peaked sharply within a narrow range of reactive metal concentrations. The largest improvement in toughness at -196° C, 7.5 times that of binary Fe-12Ni, resulted from a 0.25 atomic percent Nb addition. In Fe-12Ni-Nb alloys at low Nb addition levels, increased toughness was associated with gettering of interstitial elements; at high Nb levels, where toughness decreased, formation of intermetallic compound particles predominated. Although toughness was generally highest at the highest annealing temperature, an alloy containing 0.5 atomic percent Al displayed relatively high toughness at -196° C for all three annealing temperatures. Trends for toughness and strength at 25° C were similar to those at -196° C.

INTRODUCTION

Cryogenic pressure vessels for use in space or on the ground call for alloys that are strong, tough, and weldable. Various commercial iron (Fe) alloys are listed (ref. 1) as suitable for cryogenic service, but the technical literature contains limited

information concerning the influence of alloying elements on cryogenic toughness properties. Unfortunately, room temperature data pertaining to effects of individual elements added to a basic steel (as in ref. 2) do not necessarily provide indications of toughness behavior at lower temperatures. The prime purpose of this investigation was to systematically determine the influence of reactive metal (gettering) additions on the fracture toughness of a simple relatively pure Fe alloy at -196° C.

Iron (Fe) alloys presently utilized for cryogenic service are primarily stainless steels and alloy steels. All contain nickel (Ni), which has been recognized as effective in improving toughness in Fe. Increasing amounts of Ni lower the fracture transition temperature (ref. 3). In light of the promising results shown by Jin, et al. (ref. 4) with an Fe-12Ni-titanium (Ti) alloy, the binary alloy of Fe-12Ni, which is ductile at -196° C, was selected as the base material in this study.

When developing iron alloys for low temperature usage, one of several factors to be considered is the detrimental effect on toughness of impurity elements such as oxygen, nitrogen, and sulfur (refs. 2, 3, 5, and 6). To control this problem, it has been common practice to add to the melt reactive metal additions that combine with these impurities and thereby reduce or eliminate their detrimental effects on alloy toughness.

In this investigation the effects of minor additions of 11 eleven reactive metals on the fracture toughness and tensile properties of a ductile Fe alloy of low impurity content were examined. The reactive metals added, at levels up to 4 atomic percent (at. %), were aluminum (Al), cerium (Ce), hafnium (Hf), lanthanum (La), niobium (Nb), silicon (Si), tantalum (Ta), titanium (Ti), vanadium (V), yttrium (Y), and zirconium (Zr). Slow bend precracked Charpy fracture toughness tests and tensile tests were used to measure the influence of the reactive metal elements on the properties of Fe-12Ni at -196° and 25° C. Tests were performed on 35 alloys in three annealed conditions. Alloy microstructure and extracted particle identification were also studied.

EXPERIMENTAL PROCEDURE

Alloy Preparation

The Fe-12Ni alloys used in this investigation were prepared from vacuum processed Fe rod of 99.95 weight percent purity, electrolytic Ni chips containing less than 100 weight ppm total interstitial impurities, and 11 reactive metals. Initially, nominal 0.25 and 0.5 percent (compositions in at. % unless stated otherwise) additions of each reactive metal were evaluated. Less soluble reactive metals were added up to their solid solubility limits in Fe. Larger additions, up to 4 percent, were subsequently studied for four selected elements (Al, Nb, Ti, and V) when the initial additions

2

of 0.25 and 0.5 percent produced considerable increases in fracture toughness. Table I lists the nominal and analyzed compositions of the 35 alloys investigated and includes interstitial analyses.

The reactive metals Al, Hf, Nb, Si, and Ta contained less than 100 ppm total oxygen (O), nitrogen (N), and carbon (C). Total interstitital levels in the Ti, V, Y, and Zr starting materials were between 1000 and 5000 ppm. Cerium was added as mischmetal, which is 99.7 percent rare earth metals containing 50 to 55 percent Ce. Lanthanum was used in a hydride powder form.

Ingots were prepared by nonconsumable arc melting of 1000-gram charges in a 7.5 centimeter (cm) diameter by 3 cm deep water-cooled copper mold after evacuating and backfilling with argon to one-half the atmospheric pressure. To adequately homogenize the ingots, each alloy was given a minimum of four melts.

The ingots were hot rolled at 1100° C after annealing for 1/2 hour at that temperature. The rolling procedure included 15 percent reductions per pass and 2 rolling passes per 5 minute reheat to a sheet thickness of 7 millimeters (mm). The air-cooled sheet was sandblasted and cut into sections. The center section provided fracture toughness specimens, and an end section was rolled further at 1100° C to a 1-mm-thick sheet from which tensile specimens were stamped. The alloy tensile strengths were not materially changed by the additional reduction in thickness. As-rolled test specimens were annealed in an argon atmosphere for 2 hours at 550°, 685°, or 820° C followed by water quenching.

Evaluation

Mechanical tests. - Slow bend fracture toughness tests were performed on pre-cracked Charpy specimens. The specimens (51 mm long by 10 mm wide by 6 mm thick) were oriented longitudinally in the sheet bar with a 45° notch across the thickness (L-T crack plane orientation in ref. 6). After annealing, each specimen was fatigue cracked to an initial crack length to specimen width ratio (a/W) of approximately 0.4. Testing was conducted in a three-point bending apparatus immersed in a liquid nitrogen bath or at room temperature (fig. 1). The specimen was positioned between a 6.35-mm-diameter center roller and two similar rollers that provided a support span of 38.1 mm. A crosshead speed of 1.3 millimeters per minute (mm/min) was used. A load/deflection curve was generated on an X-Y plotter from the outputs of a load cell which supported the bend apparatus and a double cantilever clip-in displacement gage (ref. 7). The gage sensed the deflection by means of the vertical movement of a ceramic rod riding on the bend bar (fig. 1(b)).

The fracture toughness parameter K_{Icd} was determined from load/deflection

curves by the simple empirical equivalent energy method (ref. 8). This approach provides relative fracture toughness values with the use of small-size specimens; thus, it is excellently suited to a screening program employing many alloys of limited ingot size. The relation used for calculating the fracture toughness values of a slow bend precracked Charpy test specimen was

$$K_{Icd} = \frac{S \ P_2 \ \sqrt{A_1/A_2} \ f(a/W)}{BW^{3/2}}$$

where

A_1 area under curve to maximum load

A_2 area under curve to P_2

a   specimen crack depth

B   specimen thickness

f(a/W)   value of power series for a/W (given in ref. 7)

P_2 any point on linear portions of load/deflection curve

S   span for three-point bending

W   specimen width

The fracture toughness data presented are generally values obtained from single tests.

Tensile specimens stamped from the 1-mm sheet were 82 mm long in the longitudinal direction of the sheet by 15 mm wide with a 25 mm long and 6 mm wide test section. The flat surfaces of the specimens were ground or lapped. After annealing, the specimens were tensile tested in a liquid nitrogen bath or at room temperature. A constant crosshead speed of 1.3 mm/min was used.

Microstructural studies. – Longitudinal sections of annealed bend bars were examined by light microscopy. The etchant was prepared from a solution containing 33 parts water, 33 parts nitric acid, 33 parts acetic acid, and 1 part hydrofluoric acid, and it was diluted to 1 part in 20 parts of water. The slow bend fracture surfaces were viewed in a scanning electron microscope.

Second-phase particles were extracted from the matrix by electroetching in an aqueous 10 percent phosphoric acid – 10 percent tartaric acid solution with a current of about 0.02 ampere per square centimeter (A/cm^2). The particles were isolated by centrifuging. Careful rinsing was required to remove the dissolved matrix materials. An X-ray diffraction analysis of the extracted particles provided information on the crystal lattice. The emission spectrographic analysis of the particles gave a quantitative

4

measure of the metallic elements present with an estimated accuracy of ±20 percent.

Retained austenite determinations were made on electropolished bend specimens using X-ray diffraction. The volume percent austenite present was based on the integrated intensities of the austenite (111) and (220) and the ferrite or martensite (200) and (211) diffraction peaks obtained with copper K_α radiation.

RESULTS

Mechanical Behavior

Slow bend precracked Charpy fracture toughness and tensile properties of the annealed Fe-12Ni alloys at the -196° and 25° C test temperatures are presented in tables II(a) and (b) and figures 2 and 3. The Fe-12Ni alloys were tested in three annealed and quenched conditions. The three annealing temperatures (550°, 685°, and 820° C) are indicated in the $\alpha \rightleftarrows \gamma$ transformation diagram for Fe-Ni alloys (ref. 9) shown in figure 4. These represent conditions at which zero, partial, or complete transformation to austenite occurs. The structural changes resulting from these annealing temperature differences are considered in the section on microstructure.

Fracture toughness at -196° C. - Figure 2 shows the fracture toughness range (44 to 80 MPa $\sqrt{m}$; 40 to 73 ksi $\sqrt{in.}$) for the binary Fe-12Ni alloy at -196° C for the three annealing temperatures.

Initial screening of the alloy compositions was performed using 0.25 and 0.5 percent reactive metal additions. Severe cracking occurred when hot rolling ingots containing Ce (mischmetal), La, and Y in amounts exceeding their solid solubilities in α-Fe. Therefore, only small additions (up to 0.2 percent) of these reactive metals were studied here. These low concentrations of Ce, La, and Y are shown in figure 2 to generally increase the low temperature toughness.

Silicon additions to Fe-12Ni resulted in decreased toughness. This reduction in toughness was also found for Si additions up to 2.7 percent in a Ni-Cr-Mo-V steel at -196° C (ref. 10).

Additions of Zr, Hf, and Ta also have been reported to have low (<0.3 percent) solid solubilities in α-Fe (refs. 9 and 11). This may account for the increase in toughness resulting from concentrations of these reactive metals up to 0.25 percent as shown in figure 2 and the apparent decrease in toughness at levels above 0.25 percent.

Alloys containing V, Nb, Ti, and Al were studied more extensively, to concentrations as high as 4 percent, because of large increases in toughness indicated for 0.25 and 0.5 percent additions of these elements.

Toughness increased continuously with increased V content for the two highest

annealing temperatures. A maximum in toughness was indicated (fig. 2) for the 820° C annealing temperature between 1 and 2 percent V; but when annealed at 685° C, maximum toughness was apparently not attained even at 2 percent V. At the lowest annealing temperature relatively small changes in toughness were noted.

Niobium produced the highest toughness at -196° C when added to Fe-12Ni. A peak value (329 MPa $\sqrt{m}$; 299 ksi $\sqrt{in.}$) was obtained with a 0.25 percent addition of Nb for the 820° C annealed condition. This concentration of Nb also produced the maximum toughness for Fe-12Ni alloys containing Nb when annealed at 685° C. For the 550° C annealing temperature, a maximum in toughness was observed for a Nb concentration of 0.14 percent.

Titanium additions produced alloys with maximums in toughness indicated for a concentration of 0.20 percent. The highest toughness in the Fe-12Ni-Ti alloys was noted for the 685° C annealing temperature.

Aluminum added to Fe-12Ni provided alloys with good toughness at all annealing temperatures. The Fe-12Ni-Al alloys had exceptional toughness for concentrations of Al from 0.25 to 0.87 percent when annealed at 550° C. Three alloys with Al contents within this range yielded K_{Icd} values greater than 220 MPa $\sqrt{m}$ (200 ksi $\sqrt{in.}$) for this anneal condition. In contrast, alloys with other reactive metal additions generally had very poor toughness at the lowest annealing temperature.

The Fe-12Ni-Al alloys developed their highest toughness when annealed at 550° C and their lowest toughness when annealed at 820° C. In comparison, the Fe-12Ni-Nb and Fe-12Ni-Ti alloys were less tough when annealed at 550° C than at higher annealing temperatures, and peak toughness was highest in the 820° C annealed condition for the Nb additions and in the 685° C annealed condition for the Ti additions. Therefore, the annealing temperature had a strong influence on Fe-12Ni alloy toughness.

The toughness/concentration curves for V additions differ from those for the other reactive metals in that maximum toughness does not occur below 0.5 percent. Indeed, for the two lowest annealing temperatures maximum toughness apparently occurs above 2 percent V.

In summary, the toughness of the Fe-12Ni alloys at -196° C was dependent on the reactive metal, its concentration, and the annealing temperature. For those reactive metal additions more extensively studied, the general effect of increasing the concentration was to increase the toughness to a maximum. The additional reactive metal resulted in a toughness decrease to levels that approached the toughness of the original binary alloy.

Yield strength and ductility at -196° C. - Included in figure 2 are the changes in yield strength and total elongation at -196° C that resulted from additions of reactive metals to Fe-12Ni. The binary Fe-12Ni alloy exhibited yield strengths for the three

6

annealing temperatures from 827 to 889 MPa (120 to 129 ksi) and elongations from 3 to 8 percent.

Reactive metal additions of Ce, La, or Y resulted in yield strengths that were as much as 170 MPa (25 ksi) higher than indicated for Fe-12Ni with elongations increasing (e.g., from 8 to as high as 22 percent) when annealed at 550° C. Silicon additions produced alloys of poor ductility and low fracture strength. Yield strengths increased with additions of Zr, Hf, and Ta. These reactive metals also caused the elongation for most conditions to increase to a maximum at the 0.25 percent alloying level.

The remaining four reactive metals additions V, Nb, Ti, and Al displayed varying effects of concentration on yield strength and elongation. For alloys containing V or Al, peaks in the yield strengths were observed at 0.25 and 0.5 percent, respectively. These initial peaks have been described previously and were indicated to be of general occurrence in substitutional Fe-base alloys (ref. 12). No explanation for the peaks is presently available. Alloys containing Nb or Ti, annealed at 685° and 820° C, initially showed a constant yield strength or even a decrease in yield strength at very low concentrations followed by a gradual increase in yield strength as the reactive metal content increased. Alloys containing Nb and Ti and annealed at 550° C showed a linear and rapid increase in strength as the concentration increased; above about 1 percent the yield strengths of the Nb containing alloys leveled at about 1300 MPa (about 190 ksi) while the alloys containing Ti failed prior to yielding. Total elongation values of the Fe-12Ni alloys containing Nb, Ti, and Al were observed to have maximum values at about the same concentrations where maximum toughness had been indicated. Alloys containing V gradually increased in elongation as more V was added.

In summary, as reactive metal concentrations were increased, the yield strengths generally increased with some alloys displaying an initial peak. The 550° C annealed condition usually produced the highest yield strength and showed the most rapid increase in yield strength with increasing concentrations. Elongation values generally increased with small additions of reactive metals (except for Si) and showed maximums at concentrations where toughness maximums were observed.

Fracture toughness at 25° C. - The room temperature toughness of the Fe-12Ni binary alloy varied from 290 MPa $\sqrt{m}$ (264 ksi $\sqrt{in.}$) when annealed at 550° C to 96 MPa $\sqrt{m}$ (87 ksi $\sqrt{in.}$) when annealed at 820° C (fig. 3). The reactive metal additions resulted in improved room temperature toughness but mainly in the 685° and 820° C annealed conditions. Because of the high toughness of Fe-12Ni when annealed at 550° C, only Al and La additions were capable of further increasing toughness in this condition. The toughness peaks previously observed at -196° C for alloys containing 0.25 percent Nb or Ti or 0.5 percent Al are also apparent at 25° C when annealed at 685° and 820° C.

Yield strength and ductility at 25° C. - For all alloys with reactive metal contents

up to 0.5 percent and annealed at 685° and 820° C, the yield strengths at room temperature decreased from the binary Fe-12Ni values of 896 and 752 MPa (130 and 109 ksi), respectively (fig. 3). When annealed at 550° C, most of the alloys showed rapid increases in yield strength with increased reactive metal concentration. Strength levels at 25° C were 280 to 350 MPa (40 to 50 ksi) lower than at -196° C.

Elongation values at room temperature for the Fe-12Ni alloys remained relatively constant with increased concentration of reactive metals when annealed at 685° and 820° C, but these decreased when annealed at 550° C. Only Al showed a definite initial increase in elongation for the 550° C annealed condition. For additions of 0.5 percent or less, the elongation values for the lowest annealing temperature were consistently higher than for the higher annealing temperatures. Ductilities of the Fe-12Ni alloys tested at 25° C were lower, with few exceptions, than at -196° C. This anomaly is apparently related to composition since Delisle and Galibois (ref. 13) demonstrated that a low carbon martensitic steel has higher elongations at any subzero temperature than at room temperature, whereas the same steel with medium carbon content does not.

Microstructure

The addition of minor amounts, up to 0.5 percent, of the reactive metals used to modify Fe-12Ni in this investigation would not be expected to seriously affect the binary alloy microstructure. These elements were introduced to react with the interstitial impurities. Excess amounts of these reactive elements (i.e., quantities in excess of that required to "tie up" the carbon, oxygen, and nitrogen) should remain in solid solution (depending on solubility) or from compounds with Fe and/or Ni. The principal changes to be observed from these minor additions should be due to precipitation of interstitial and intermetallic compounds. More evident would be the microstructural differences that result from heat treatments involving phase transformations.

The Fe-12Ni alloys were tested in three annealed and quenched conditions. Figure 4 shows schematically the $\alpha \rightleftarrows \gamma$ transformation diagram for Fe-Ni alloys found on continuous heating and cooling. The relative positions of the three 2-hour annealing temperatures used in this investigation are indicated for the 12 percent Ni content. Hot rolling Fe-12Ni at 1100° C takes place in the austentite (γ) region. On cooling, this FCC structure transforms to the α-phase, a BCC structure. Based on the isothermal transformation diagram for 9Ni steel (refs. 14 and 15), air cooling should be sufficiently slow to produce a microstructure consisting mainly of ferrites plus carbide and austentite. However, the low carbon content of the present Fe-12Ni alloys would necessarily mean a very limited amount of carbide could form. The 550° C anneal followed by water quenching provides a stress-relief-type operation with no transformation

taking place. On heating for 2 hours within the $\alpha \rightarrow \gamma$ transformation zone, the amount of transformation product varies with the annealing temperature. When annealed at 685° C, about one-half of the α in the hot-rolled binary Fe-12Ni alloy reverts to γ which, on quenching, transforms to martensite producing a mixed microstructure of ferrite and martensite. Annealing at 820° C completely transforms Fe-12Ni to γ which forms martensite on quenching. Typical microstructures of binary Fe-12Ni resulting from these annealing conditions are shown in the photomicrographs in figure 5.

In general, the microstructural phases indicated as present in the Fe-12Ni binary for the previous annealing conditions are also exhibited in alloys containing up to 0.5 percent additions of the reactive metals. As typical examples, the effects of 0.5 percent Al and 0.25 percent Nb additions on the Fe-12Ni microstructures are shown in figures 6 and 7. (Likewise, the temperature range for $\alpha \rightarrow \gamma$ transformation in Fe-12Ni, as indicated by differential thermal analysis measurements, did not change appreciably due to the minor additions of reactive metals used in this investigation.)

Grain size measurements of the 550° C annealed materials indicated that the ternary alloys had average grain diameters approximately one-half the 75-micrometer (μm) size determined for the Fe-12Ni binary alloy. Retained austenite was generally not present in these alloys, but X-ray diffraction results indicated that as much as 2.4 volume percent was detected in several of the alloys when annealed at 550° C.

Figure 8 shows typical transmission electron micrographs of the Fe-12Ni alloys. An elongated subgrain structure was generally observed. The binary Fe-12Ni alloy (fig. 8(a)) had relatively few dislocations, and its subgrain boundaries were poorly defined. The Fe-12Ni-0.5Al alloy (fig. 8(b)) displayed sharper subgrain boundaries and a greater density of dislocations. The addition of 0.25 percent Nb to Fe-12Ni (fig. 8(c)) yielded a microstructure wherein the boundaries were obscured by dense dislocation tangles. The effect of a higher annealing temperature on the latter alloy is shown in figure 8(d) to have produced subgrains that were of a larger more equiaxed character; many of the dislocation tangles were retained at the subgrain boundaries, but well-defined dislocations were observed within the subgrains. Generally precipitate particles were not encountered except in those alloys containing strong carbide-forming additions such as Hf and Ta.

From a comparison of the dislocation characteristics and the toughness values given in (a) and (c) of figure 8, it appears that substructure plays a minor role in fracture toughness.

To examine the characteristics and compositions of the particles in the Fe-12Ni alloys, aging experiments were conducted and chemical extractions of particles were attempted. Aging the hot-rolled alloys at 550° C is shown in figure 9 to cause hardening in Fe-12Ni-0.5Nb and Fe-12Ni-0.5Ti alloys but only gradual softening in Fe-12Ni-1Al. The lack of an aging response is assumed to reflect no nucleation or growth of precipi-

9

tates in the Fe-12Ni-1Al alloy. In contrast, at higher levels of Ni and Al, Speich (ref. 16) found intense hardening on aging of Fe-20Ni-5.4Al at 500° C but no visible precipitation.

Particles were extracted chemically from the Fe-12Ni alloys containing Al, Nb, and Ti. Only the extracted particles from the Fe-12Ni-Nb alloys were not oxidized during extraction and could be identified by X-ray diffraction. The results of analyses of the Nb-containing particles by X-ray diffraction and emission spectrography are given in table III. These results are interpreted to indicate that Nb additions combine initially with the interstitial impurities oxygen, nitrogen, and carbon. After gettering the interstitial elements is completed and when the solubility of Nb in the matrix is exceeded, the excess Nb combines with Fe and Ni to form a hexagonal phase with a diffraction pattern similar to that of Fe_2Nb. The metallic element analyses of the particles extracted from the alloy containing 2 percent Nb ranged from 60 to 65 weight percent Fe + Ni. If Fe were substituted for the Ni present, then the particle composition would be located in the Fe-rich portion of the ϵ-phase (which includes Fe_2Nb) for the Nb-Fe equilibrium diagram shown in reference 11. Therefore, based on these analyses, this hexagonal phase is considered to be $(Fe, Ni)_{\sim 2}Nb$. The ratio of Fe to Ni for the particles derived from the Fe-12Ni-2Nb alloy averaged 6.5, which compares closely with the Fe/Ni ratio of the alloy itself.

Fractographic examination of the fracture toughness test specimens revealed that plastic fracture (dimpled rupture) occurred in varying degrees in the Fe-12Ni alloys, being most evident in the toughest materials. Figure 10 shows the change in fracture character in Fe-12Ni-0.25Nb with different annealing temperatures. Large amounts of cleavage fracture are visible in the 550° C annealed condition (fig. 10(a)) which also had relatively low cryogenic toughness. Conversely, a large amount of dimpled rupture is evident in the 820° C annealed material (fig. 10(c)) which had the highest toughness at -196° C. In figure 11, the fracture surfaces of Fe-12Ni-0.5Al show a uniformly high level of dimpled rupture for all three annealing temperatures. Fracture toughness at -196° C was uniformly high for three annealing conditions for this alloy. The formation of voids is usually recognized as the first stage of plastic fracture, and, in many cases, the initiation of voids is attributed to inclusions (refs. 17 and 18). Inclusions are clearly visible in the larger voids of the Fe-12Ni-Hf alloys annealed at 820° C (fig. 12). This alloy had moderate toughness at -196° C.

DISCUSSION

The preceding results have shown that minor amounts of reactive metals added to Fe-12Ni exert a strong influence on the low temperature fracture toughness. Tensile

ductility was similarly affected although no direct relation between elongation and toughness was apparent. Yield strength increases were usual with alloying additions up to 0.5 percent, especially in the 550° C annealed condition. It is apparent that the low temperature toughness in low impurity Fe-12Ni alloys is greatly affected by all three variables studied: (1) the reactive metal added, (2) its concentration, and (3) heat treatment. The effects of these variables are discussed in the next two sections.

Effects of Reactive Metal Additions

Of the 11 reactive metals tested, only additions of Si did not improve the toughness of Fe-12Ni at -196° C. Five of the alloying elements (Al, La, Ta, Ti, and V) provided definite increases in the low temperature toughness at all three annealing temperatures. The reactive metals were tentatively ranked as to their effectiveness in increasing the toughness of Fe-12Ni at -196° C. Ranking was accomplished by using the average fracture toughness for the three annealing conditions at the optimum concentration for each reactive metal. This indicated the following order of decreasing effectiveness: Al, Ta, V, Ti, Nb, La, Hf, Y, Ce (mischmetal), and Zr.

For comparison, figure 13 presents the fracture toughness improvements resulting from the six most effective additions when tested at -196° and 25° C. The improvement was determined from the ratio of ternary alloy toughness to binary Fe-12Ni toughness. For example, the nominal 0.1 percent La alloy had a toughness (at -196° C when annealed at 550° C) of 201 MPa$\sqrt{m}$ (183 ksi$\sqrt{in.}$) compared to 80 MPa$\sqrt{m}$ (73 ksi$\sqrt{in.}$) for the binary Fe-12Ni alloy, a ratio of about 2.5 improvement of fracture toughness. While this alloy displayed similar or greater improvement at the higher annealing temperatures, it was observed that ingots containing La (1) suffered a loss in La content during melting (as observed in ref. 19), (2) developed a white powdery coating on standing, and (3) fractured during rolling at La contents greater than 0.1 percent (limit of solid solubility in α-iron). These features indicated some practical disadvantages to the use of La.

Niobium was the most effective toughness improver at the highest annealing temperature: the Fe-12Ni-0.25Nb alloy being about 7.5 times tougher than Fe-12Ni at -196° C. However, in effectiveness at the 685° C annealing temperature, Nb ranked below Ti, V, Ta, and Al, and at the lowest annealing temperature (550° C), the Nb additions produced no appreciable change in the toughness of Fe-12Ni.

Both Ti and Ta exhibited better toughness than V at the intermediate 685° C annealing temperature. But at the 550° and 820° C annealing temperatures, V performed better and may possibly show greater toughness improvement at V levels greater than 2 percent.

Aluminum provided the best low temperature toughness improvement at the 550° C annealing temperature, 3.5 times the toughness of binary Fe-12Ni. The 0.5 percent Al addition also had the unique feature of producing uniformly high toughness improvement for all three annealing temperatures.

Figure 13 also shows that the reactive metals were considerably less effective in improving the toughness of the base material at room temperature than at -196° C. This was due primarily to the higher toughness of the Fe-12Ni binary alloy at 25° C, especially when annealed at 550° C. Consequently, only Al and La increased the room temperature toughness at the lowest annealing temperature, providing as much as 20 percent improvement. However, at the higher annealing temperatures, Nb, Ta, Ti, and V additions produced notable changes; for example, the Fe-12Ni toughness at 25° C was improved by 100 to 150 percent.

Annealing Effects

In figure 14 the relation of fracture toughness at -196° C to annealing temperature is shown for the Al, Nb, and Ti additions to Fe-12Ni at the concentrations which produced the highest toughness. Since the three 2-hour annealing temperatures represent zero, partial, and complete transformation of ferrite to austenite, it is actually the effects of structural changes occurring during annealing (and subsequent water quenching) that are being related to the fracture toughness.

It should be noted that the Fe-12Ni binary alloy showed small decreases in toughness as the annealing temperature was increased. A much higher toughness with almost parallel dependence was displayed by the alloy containing 0.5 percent Al. Alloyed with 0.25 percent Nb, Fe-12Ni is shown to increase rapidly in toughness on passing through the $\alpha \rightarrow \gamma$ transformation region. Therefore, the effect of Al is opposite to that of Nb: the peak toughness of the Al-containing alloy resulted from the 550° C annealing temperature (untransformed ferrite structure), while the peak toughness of the Nb-modified alloy resulted from the 820° C annealing temperature (where complete transformation to austenite occurred). Although Ti additions at higher concentrations indicated toughness/annealing temperature relations similar to Nb additions, the maximum toughness for the 0.25 percent Ti alloy occurred at the 685° C annealing temperature.

Interestingly, these elements and the other reactive metal additions tend to group themselves in their toughness response to the three annealing temperatures. Based on the present data, the reactive metal additions can be grouped according to the annealing temperature at which the highest toughness was observed. Maximum toughness was achieved in the base material Fe-12Ni when annealed at 550° C (α region); similar results occurred when optimum amounts of Al, Ce, or La were added. Peak toughness

12

was achieved with the alloys containing Hf, Ti, V, or Y when these alloys were annealed at 685° C ($\alpha + \gamma$ region). Maximum toughness at the 820° C annealing temperature (γ region) was displayed for the alloys containing Nb, Ta, or Zr.

Photomicrographs of these alloys were compared to determine if the previous group responses corresponded to the observed alloy microstructures. It can be seen in figures 6 and 7 that the Fe–12Ni optical microstructures were not basically changed by the addition of 0.5 percent Al. The alloys containing Ce and La had somewhat finer grained structures that made them difficult to relate with the Fe–12Ni. The 0.1 percent Y alloy, although previously grouped under the 685° C annealing temperature for peak toughness, had microstructures that closely resembled those of the binary Fe–12Ni. All other reactive metal additions produced structures which differed considerably from that of the original base material in the lack of platelet streaking in the 550° C anneal, the size and greater degree of mixing of the platelets developed by the 685° C anneal, and the reduced amount of inscription within the martensite lath resulting from the 820° C anneal. Thus, it is concluded that there is not a direct correlation between microstructures resulting from annealing at the three temperatures and grouping of alloys with different reactive metals based on their peak fracture toughness.

Comparison with Commercial Alloys

This initial effort to improve the low temperature toughness of the Fe alloys investigated the effects on Fe–12Ni. Figure 15 compares the –196° C fracture toughness and yield strength results of the Fe–12Ni alloys with those of various commercial alloys. (The data on the commercial alloys were obtained through the same testing methods used for the experimental alloys.) Also included are data from an experimental Fe–12Ni–0.3Ti alloy (described as specimen 1A by Jin, et al. in ref. 20) which was heat treated at 730° C to yield a microstructure and fracture toughness similar to that of our Fe–12Ni–0.25Ti alloy annealed at 820° C. Further improvements in toughness for this alloy have been attained through grain refinement.

Low toughness has usually been associated with alloys of high strength, such as D6AC and 9Ni–4Co steels. The maraging steels with a higher Ni content (such as the 18Ni, 200–grade steel indicated in fig. 15) have greater toughness in the high strength range. In the medium strength range, 9Ni steel typifies a material of good toughness, while 304 stainless steel represents the greater toughness usually exhibited in a lower strength steel. In this spectrum of Fe alloys it can be seen that the Fe–12Ni binary alloy provides relatively low toughness in the medium strength range. However, through the addition of reactive metals the low temperature toughness of this binary

alloy has been increased to levels as much as 80 percent higher than 9Ni steel at a comparable strength level.

CONCLUDING REMARKS

The large improvements in toughness indicated in this investigation emphasize the value of adding reactive metals to iron alloys. Optimum concentrations of reactive metals can eliminate the detrimental effects of interstitial impurity elements that limit low temperature toughness. Optimum concentrations, however, may change with the amount of impurity present – a factor which was not studied here. Also, the presence of other contaminants such as sulfur and phosphorus in larger amounts may complicate the results and reduce the effectiveness of the reactive metals in developing the high toughness values recorded here.

Control of reactive metal concentration is an important consideration. Some metal loss may be expected as was observed for the rare earth element additions. However, it would appear more practical (as may be noted from fig. 2) to use reactive metal additions, such as Al and V, that provide high toughness over relatively broad concentration ranges rather than those, such as Nb, Ta, and Ti, which exhibit high toughness only within very narrow concentration ranges.

These striking improvements in fracture toughness have been accomplished in Fe-12Ni, an alloy of moderate strength. Alloys in this strength category, such as 9Ni steel, already have relatively high toughness at -196° C. Therefore, higher strength alloys with these high toughness values are desired to achieve maximum usefulness. Thus, we have set a future goal of achieving toughness in the vicinity of 220 MPa $\sqrt{m}$ (200 ksi $\sqrt{in.}$) in alloys with yield strengths at -196° C of the order of 1400 MPa (200 ksi). Since strength is generally gained at the expense of toughness, it is likely that the best Fe-12Ni alloys listed here have an adequate reserve of toughness to attain this goal through modifications in alloy chemistry and/or processing to achieve yield strength values near 1400 MPa (200 ksi).

SUMMARY OF RESULTS

The slow bend precracked Charpy fracture toughness and tensile test behavior of arc-melted and hot-rolled Fe-12Ni alloys containing up to 4 atomic percent reactive metal additions were evaluated at -196° and 25° C after quenching from three annealing temperatures with the following results:

1. The fracture toughness of the Fe-12Ni alloys at -196° C was dependent on the reactive metal added, its concentration, and the heat treatment.

2. Reactive metal additions that increased the -196° C fracture toughness of Fe-12Ni to K_{Icd} values greater than 220 MPa$\sqrt{m}$ (200 ksi$\sqrt{in.}$) were Al, Nb, Ta, Ti, and V. Less effective additions were Ce (as mischmetal), Hf, La, Y, and Zr. Only Si additions did not improve the low temperature toughness of Fe-12Ni.

3. Fracture toughness values peaked sharply within a narrow concentration range for most of the additions. For example, a maximum in toughness was observed at both -196° and 25° C for Ti additions less than 0.5 atomic percent for all three annealing conditions. Vanadium was an exception in that toughness continued to increase with concentrations up to 2 atomic percent (the maximum level studied).

4. The addition of 0.25 atomic percent Nb resulted in the largest toughness improvement at -196° C – namely, 7.5 times the Fe-12Ni toughness values for the 820° C anneal; this alloy addition, however, gave no improvement in toughness for the 550° C anneal. A 0.5 atomic percent Al addition provided relatively high (3.5- to 5-fold range) toughness improvement at -196° C for all three annealing conditions. Yield strengths at -196° C were generally improved by the reactive metal additions and, for the previous alloys, ranged from about 900 to 1100 MPa (130 to 160 ksi).

5. Toughness variations with Nb concentration appear to be associated at low addition levels with the gettering of interstitials followed by intermetallic compound formation as Nb content is increased.

6. Room temperature toughness and tensile results show trends similar to those at -196° C but with considerably lower (or even negative) toughness improvements.

Lewis Research Center,
    National Aeronautics and Space Administration,
        Cleveland, Ohio, March 4, 1976,
            506-16.

REFERENCES

1. Metal Progress Databook. Am. Soc. Metals, 1975, p. 118.

2. Rinebolt, J. A.; and Harris, W. J., Jr.: Effect of Alloying Elements on Notch Toughness of Pearlitic Steels. Trans. Am. Soc. Metals, vol. 43, 1951, pp. 1175-1214.

3. Steigerwald, E. A.; and Vishnevsky, C.: Literature Survey on the Influence of Alloy Elements on the Fracture Toughness of High Strength Steels. TRW, Inc. (AMMRC-CR-67-13(F); AD-665432), 1968.

4. Jin, S.; Morris, J. W., Jr.; and Zackey, V. F.: An Iron-Nickel-Titanium Alloy with Outstanding Toughness at Cryogenic Temperature. Cryogenic Engineering Conference. Plenum Press, 1974, pp. 379-384.

5. Rees, W. P.; and Hopkins, B. E.: Intergranular Brittleness in Iron-Oxygen Alloys. J. Iron and Steel Inst., vol. 172, pt. 4, Dec. 1952, pp. 403-409.

6. Pickering, F. B.: The Effect of Composition and Microstructure on Ductility and Toughness. Symposium: Toward Improved Ductility and Toughness, Climax Molybdenum Development Co. (Japan) Ltd., 1971, pp. 9-31.

7. Standard Method of Test for Plane-Strain Fracture Toughness of Metallic Materials. Standard E399-74, Am. Soc. for Testing and Materials, 1974.

8. Witt, F. J.; and Mager, T. R.: A Procedure for Determining Bounding Values on Fracture Toughness K_{Ic} at any Temperature. ORNL-TM-3894, Oakridge Natl. Lab., 1972.

9. Hansen, Max: Constitution of Binary Alloys. McGraw-Hill, 1958.

10. Vishnevsky, C.; and Steigerwald, E. A.: Influence of Alloying Elements on the Low-Temperature Toughness of Martensitic High Strength Steels. Trans. Am. Soc. Metals, vol. 62, no. 2, June 1969, pp. 305-317.

11. Elliott, Rodney P.: Constitution of Binary Alloys. First Supplement, McGraw-Hill Book Co., Inc., 1965.

12. Leemans, D.; and Fine, M. E.: Solid Solution Softening and Strain-Rate Sensitivity of Fe-Re and Fe-Mo Alloys. Met. Trans., vol. 5, no. 6, June 1974, pp. 1331-1336.

13. Delisle, G.; and Galibois, A.: Microstructural Studies of Tempered Extra-Low Carbon Steels and Their Effectiveness in Interpreting Tempered Martensite Brittleness. Microstructural Science, Vol. I, Robert J. Gray and James L. McCall, eds., American Elsevier Publishing Co., Inc., 1974, pp. 91-112.

14. 9% Nickel Steel for Low Temperature Service. Bulletin A-263, International Nickel Co., Inc., 1973.

15. Marschall, C. W.; Hehemann, R. F.; and Troiano, A. R.: The Characteristics of 9% Nickel Low Carbon Steel. Trans. Am. Soc. Metals, vol. 55, 1962, pp. 135-148.

16

16. Speich, G. R.: Age Hardening of Fe–20 Pct Ni Martensites. Trans. AIME, vol. 227, Dec. 1963, pp. 1426-1432.

17. Sullivan, C. P.: A Review of Some Microstructural Aspects of Fracture in Crystalline Materials. Bulletin 122, Welding Research Council, 1967.

18. Cox, T. B.; and Low, J. R., Jr.: An Investigation of the Plastic Fracture of AISI 4340 and 18 Nickel – 200 Grade Maraging Steels. Met. Trans., vol. 5, no. 6, June 1974, pp. 1457-1470.

19. Gautschi, Rudolph H.; and Langenberg, Frederick C.: Effect of Rare-Earth Additions on Some Stainless Steel Melting Variables. Trans. AIME, vol. 218, Feb. 1960, pp. 128-132.

20. Jin, S.; Hwang, S. K.; and Morris, J. W., Jr.: Comparative Fracture Toughness of an Ultrafine Grained Fe-Ni Alloy at Liquid Helium Temperature. Met. Trans., Pt. A – Phys. Metall. Mat. Sci., vol. 6A, no. 8, Aug. 1975, pp. 1569-1575.

TABLE I. – COMPOSITIONS OF Fe-12Ni ALLOYS USED IN THIS STUDY

Nominal composition, at.%	Analyzed composition, at.%		Interstitial content, ppm (by weight) [of 820° C anneal, -196° C bend test specimens]		
	Ni	Addition	O	N	C
Fe-12Ni	11.9	--------	12	7	162
Fe-12Ni-0.25Al	11.8	0.24Al	18	7	151
Fe-12Ni-0.5Al	11.9	.49Al	20	8	158
Fe-12Ni-1Al	12.3	.87Al	34	19	96
Fe-12Ni-2Al	12.7	1.94Al	26	20	94
Fe-12Ni-4Al	12.0	4.00Al	44	57	432
Fe-12Ni-0.1Ce[a]	12.7	0.1Ce[a]	34	28	411
Fe-12Ni-0.25Hf	11.6	0.24Hf	76	30	48
Fe-12Ni-0.5Hf	12.0	.50Hf	83	22	58
Fe-12Ni-0.1La	11.9	0.04La	64	10	35
Fe-12Ni-0.15Nb	12.2	0.14Nb	184	101	14
Fe-12Ni-0.2Nb	12.1	.17Nb	172	76	14
Fe-12Ni-0.25Nb[b]	12.1	.25Nb	22	10	82
Fe-12Ni-0.5Nb	11.9	.46Nb	11	10	92
Fe-12Ni-1Nb	11.8	.97Nb	239	24	18
Fe-12Ni-2Nb	12.4	1.50Nb	121	25	22
Fe-12Ni-3Nb	12.9	3.00Nb	146	30	20
Fe-12Ni-0.25Si	12.1	0.26Si	138	14	16
Fe-12Ni-0.5Si	12.2	.44Si	176	14	18
Fe-12Ni-0.1Ta	12.0	0.10Ta	14	20	264
Fe-12Ni-0.25Ta	12.0	.24Ta	14	22	278
Fe-12Ni-0.35Ta	11.9	.34Ta	11	18	178
Fe-12Ni-0.25Ti	12 4	0.20Ti	61	12	18
Fe-12Ni-0.5Ti	12.2	.47Ti	68	13	25
Fe-12Ni-1Ti	12.2	.99Ti	63	28	36
Fe-12Ni-2Ti	11.9	1.93Ti	94	24	40
Fe-12Ni-3Ti	12.6	3.21Ti	93	30	46
Fe-12Ni-0.25V	12.3	0.27V	43	24	362
Fe-12Ni-0.5V	11.9	.55V	9	28	214
Fe-12Ni-1V	12.0	1.00V	24	31	184
Fe-12Ni-2V	12.0	1.99V	25	44	150
Fe-12Ni-0.1Y	12.2	0.07Y	45	31	164
Fe-12Ni-0.25Y	11.7	.20Y	52	44	96
Fe-12Ni-0.25Zr	12.0	0.24Zr	106	30	105
Fe-12Ni-0.5Zr	11.7	.48Zr	99	12	88

[a]Mischmetal containing 50 to 55 percent cerium plus other rare
   earth metals.
[b]Additional analyses on Fe-12Ni-0.25Nb indicated 20 ppm P,
   16 ppm S, 63 ppm Si.

TABLE II. – FRACTURE TOUGHNESS AND TENSILE PROPERTIES OF Fe-12Ni ALLOYS

(a) At -196° C

Nominal compositions of Fe-12Ni alloys, at.%	550° C annealed condition							685° C annealed condition							820° C annealed condition						
	Yield strength		Ultimate tensile strength		Elonga-tion, %	Fracture toughness, K_{Icd}		Yield strength		Ultimate tensile strength		Elonga-tion, %	Fracture toughness, K_{Icd}		Yield strength		Ultimate tensile strength		Elonga-tion, %	Fracture toughness, K_{Icd}	
	MPa	ksi	MPa	ksi	%	MPa √m	ksi √in.	MPa	ksi	MPa	ksi	%	MPa √m	ksi √in.	MPa	ksi	MPa	ksi	%	MPa √m	ksi √in.
Fe-12Ni	827	120	876	127	8	80	73	889	129	924	134	3	66	60	862	125	951	138	3	44	40
Fe-12Ni-0.25Al	827	120	938	136	20	249	227	924	134	1069	155	6	173	157	869	126	1076	156	13	129	117
Fe-12Ni-0.5Al	896	130	945	137	28	b284	a258	1103	160	1193	173	10	a237	a216	1041	151	1117	162	15	a219	a199
Fe-12Ni-1Al	889	129	931	135	23	293	267	883	128	1041	151	9	95	86	958	139	1000	145	9	63	57
Fe-12Ni-2Al	1227	178	1255	182	8	41	37	1027	149	1124	163	8	113	103	972	141	1048	152	12	74	67
Fe-12Ni-4Al	1351	196	2668	205	2	24	22	1186	172	1351	196	11	118	107	1117	162	1248	181	12	79	72
Fe-12Ni-0.1Ce	903	131	1041	151	22	127	116	1062	154	1179	171	9	147	134	1020	148	b1062	b154	0	33	30
Fe-12Ni-0.25Hf	951	138	1048	152	17	79	72	945	137	1048	152	8	211	192	779	113	951	138	16	36	124
Fe-12Ni-0.5Hf	986	143	1027	149	18	55	50	786	114	958	139	5	69	63	931	135	993	144	14	103	94
Fe-12Ni-0.1La	834	121	917	133	19	201	183	965	140	1055	153	14	165	150	924	134	1014	147	12	165	150
Fe-12Ni-0.15Nb	938	136	986	143	12	197	179	945	137	1076	156	8	152	138	869	126	965	140	18	213	194
Fe-12Ni-0.2Nb	972	141	1000	145	12	149	136	965	140	1124	163	14	153	139	855	124	917	133	13	204	186
Fe-12Ni-0.25Nb	1041	151	1082	157	14	80	73	965	140	1055	153	11	197	179	917	133	1020	148	16	329	299
Fe-12Ni-0.5Nb	1172	170	1207	175	9	59	54	917	133	1103	160	12	164	149	979	142	1048	152	12	246	224
Fe-12Ni-1Nb	1365	198	1413	205	7	47	43	993	144	1138	165	13	113	103	979	142	1096	159	13	127	116
Fe-12Ni-2Nb	1310	190	1386	201	5	37	34	1055	153	1200	174	12	90	82	1103	160	1282	186	12	98	89
Fe-12Ni-3Nb	1331	193	1400	203	3	44	40	1089	158	1261	183	9	76	69	1014	147	1172	170	10	89	81
Fe-12Ni-0.25Si	----	---	b565	b82	0	25	23	----	---	b524	b76	0	23	21	876	127	951	138	2	37	34
Fe-12Ni-0.5Si	----	---	b841	b122	0	26	24	----	---	b800	b116	0	27	25	876	127	945	137	2	38	35
Fe-12Ni-0.1Ta	1138	165	1193	173	16	64	58	1110	161	1220	177	10	110	100	1014	147	1096	159	13	47	43
Fe-12Ni-0.25Ta	1055	153	1096	159	18	180	164	972	141	1062	154	16	229	208	827	120	931	135	15	259	236
Fe-12Ni-0.35Ta	1179	171	1200	174	11	118	107	993	144	1082	157	13	213	194	896	130	979	142	12	269	245
Fe-12Ni-0.25Ti	827	120	924	134	20	127	116	889	129	958	139	15	275	250	848	123	924	134	15	a211	a192
Fe-12Ni-0.5Ti	1034	150	1117	162	14	60	55	889	129	1014	147	9	178	162	807	117	951	138	13	189	172
Fe-12Ni-1Ti	1282	186	1344	195	9	35	32	862	125	1082	157	11	104	95	869	126	1014	147	11	a131	a119
Fe-12Ni-2Ti	←—— Brittle ——→					20	18	958	139	1248	181	14	77	70	993	144	1076	156	11	a118	a107
Fe-12Ni-3Ti	←—— Brittle ——→					18	16	----	---	b703	b102	0	41	37	1117	162	1241	180	9	64	58
Fe-12Ni-0.25V	1213	176	1289	187	15	80	73	1089	158	1213	176	10	186	169	1076	156	1186	172	9	87	79
Fe-12Ni-0.5V	1082	157	1145	166	15	76	69	1048	152	1145	166	12	224	204	1062	154	1165	169	13	162	147
Fe-12Ni-1V	965	140	1041	151	17	88	80	986	143	1110	161	12	251	228	1007	146	1089	158	12	260	237
Fe-12Ni-2V	1007	146	1069	155	21	112	102	1014	147	1096	159	10	288	262	1014	147	1110	161	14	247	225
Fe-12Ni-0.1Y	862	125	896	130	18	51	46	1048	152	1124	163	12	143	130	979	142	1124	163	10	137	125
Fe-12Ni-0.25Y	834	121	883	128	19	74	67	972	141	1048	152	11	103	94	979	142	1076	156	9	111	101
Fe-12Ni-0.25Zr	910	132	958	139	14	78	78	931	135	1000	145	10	67	61	883	128	1020	148	12	99	90
Fe-12Ni-0.5Zr	938	136	972	141	16	71	65	965	140	1020	148	10	57	52	938	136	1007	146	11	80	73

a Average of two tests.
b Fracture strength.

TABLE II. – Concluded.

(b) At 25° C

Nominal compositions of Fe-12Ni alloys, at.%	550° C annealed condition							685° C annealed condition							820° C annealed condition						
	Yield strength		Ultimate tensile strength		Elongation, %	Fracture toughness, K_{Icd}		Yield strength		Ultimate tensile strength		Elongation, %	Fracture toughness, K_{Icd}		Yield strength		Ultimate tensile strength		Elongation, %	Fracture toughness, K_{Icd}	
	MPa	ksi	Mpa	ksi		MPa $\sqrt{m}$	ksi $\sqrt{in.}$	MPa	ksi	MPa	ksi		MPa $\sqrt{m}$	ksi $\sqrt{in.}$	MPa	ksi	MPa	ksi		MPa $\sqrt{m}$	ksi $\sqrt{in.}$
Fe-12Ni	565	82	607	88	17	[a]290	[a]264	903	131	924	134	6	109	99	752	109	862	125	4	96	87
Fe-12Ni-0.25Al	593	86	627	91	18	357	325	731	106	855	124	5	143	130	683	99	779	113	4	122	111
Fe-12Ni-0.5Al	607	88	641	93	19	320	291	889	129	1034	150	4	188	171	696	101	807	117	5	180	164
Fe-12Ni-1Al	586	85	627	91	14	326	297	593	86	786	114	2	163	148	614	89	758	110	3	147	134
Fe-12Ni-2Al	965	140	986	143	7	205	187	717	104	834	121	4	243	221	676	98	786	114	5	177	161
Fe-12Ni-4Al	1207	175	1379	200	9	67	61	903	131	1076	156	10	73	66	848	123	1000	145	6	76	69
Fe-12Ni-0.1Ce	607	88	703	102	18	143	130	793	115	938	136	3	118	107	772	112	896	130	7	88	80
Fe-12Ni-0.25Hf	689	100	731	106	14	129	117	738	107	827	120	6	112	102	565	82	676	98	5	122	111
Fe-12Ni-0.5Hf	683	99	738	107	13	114	104	627	91	710	103	6	102	93	579	84	669	97	6	116	106
Fe-12Ni-0.1La	552	80	607	88	18	338	308	662	96	765	111	5	125	114	593	86	648	94	6	132	120
Fe-12Ni-0.15Nb	634	92	669	97	11	220	200	572	83	683	99	7	169	154	517	75	634	92	6	200	182
Fe-12Ni-0.2Nb	662	96	689	100	9	227	207	586	85	689	100	4	174	158	524	76	614	89	7	193	176
Fe-12Ni-0.25Nb	758	110	807	117	11	277	252	621	90	703	102	5	213	194	593	86	689	100	8	242	220
Fe-12Ni-0.5Nb	862	125	903	131	8	246	224	655	95	731	106	6	204	186	614	89	696	101	6	196	178
Fe-12Ni-1Nb	1041	151	1055	153	5	100	91	676	98	793	115	6	116	106	696	101	779	113	7	129	117
Fe-12Ni-2Nb	1034	150	1076	156	3	65	59	696	101	827	120	5	74	67	600	87	800	116	6	98	89
Fe-12Ni-3Nb	1041	151	1089	158	3	55	50	717	104	876	127	6	64	58	662	96	800	116	7	75	68
Fe-12Ni-0.25Si	545	79	579	84	16	← n.d. →		696	101	731	106	2	← n.d. →		607	88	696	101	4	46	42
Fe-12Ni-0.5Si	558	81	593	86	17	278	253	710	103	738	107	4	41	37	600	87	676	98	5	42	38
Fe-12Ni-0.1Ta	820	119	876	127	11	98	89	738	107	841	122	4	159	145	648	94	752	109	3	167	152
Fe-12Ni-0.25Ta	738	107	758	110	5	282	257	614	89	696	105	4	180	164	565	82	648	94	2	255	232
Fe-12Ni-0.35Ta	814	118	841	122	10	244	222	621	90	731	106	5	227	207	545	79	634	92	8	275	250
Fe-12Ni-0.25Ti	593	86	634	92	14	289	263	614	89	641	93	8	276	251	565	82	648	94	6	202	184
Fe-12Ni-0.5Ti	793	115	827	120	7	188	171	662	96	696	101	4	169	154	586	85	669	97	2	177	161
Fe-12Ni-1Ti	903	131	1014	147	4	156	142	531	77	724	105	2	171	156	476	69	641	93	3	179	163
Fe-12Ni-2Ti	1338	194	1420	206	3	45	41	683	99	903	131	8	157	143	641	93	772	112	5	131	119
Fe-12Ni-3Ti	← Brittle →							676	98	938	136	5	131	119	703	102	869	126	5	154	140
Fe-12Ni-0.25V	862	125	917	133	7	111	101	807	117	945	137	4	222	202	752	109	903	131	5	203	185
Fe-12Ni-0.5V	710	103	765	111	10	168	-153	703	102	807	117	4	186	169	758	110	814	118	6	173	157
Fe-12Ni-1V	655	95	703	102	11	264	240	648	94	745	108	4	189	172	696	101	814	118	4	190	173
Fe-12Ni-2V	676	98	717	104	12	285	259	641	93	738	107	5	225	205	689	100	807	117	2	187	170
Fe-12Ni-0.1Y	586	85	621	90	12	102	93	765	111	869	126	3	90	82	717	104	820	119	4	99	90
Fe-12Ni-0.25Y	545	79	586	85	14	79	72	731	106	772	112	2	85	77	662	96	752	109	3	81	74
Fe-12Ni-0.25Zr	641	93	676	98	13	137	125	607	88	703	102	4	101	92	572	83	669	97	4	103	94
Fe-12Ni-0.5Zr	655	95	696	101	10	104	95	627	91	717	104	3	91	83	593	86	696	101	3	82	75

[a]Average of two tests.

TABLE III. – ANALYSES OF EXTRACTED PARTICLES FROM Fe-12Ni-Nb TOUGHNESS
TEST SPECIMENS

Nominal Nb content, at.%	Annealing temperature, °C	X-ray diffraction analysis phases detected				Emission spectrographic analysis			
		NbO_2	NbN	NbC	Hexagonal phase[a]	Metallic element content of particles, wt.% of total (Fe + Ni + Nb)			Recovery, %
						Fe	Ni	Nb	
0.15	550	VS[b]	S[c]	---	-----	0.7	0.3	99.0	63
	820	VS	S	---	-----	2.5	.6	96.9	72
.25	550	---	--	VS	-----	57.9	7.5	34.7	37
	820	---	--	VS	-----	24.9	1.2	73.9	58
.5	550	---	--	VS	VVW[d]	19.9	5.5	74.7	60
	820	---	--	S	S	51.5	6.6	41.9	62
1	550	---	--	---	VS	59.3	8.4	32.3	80
	550	---	--	---	VS	55.2	7.9	36.9	84
2	550	---	--	---	VS	50.3	9.9	39.7	96
	550	---	--	---	VS	56.1	8.8	35.2	84
	820	---	--	---	VS	55.2	6.9	37.9	87

[a]X-ray diffraction lines match those for Fe_2Nb. This is the ϵ-phase in the Nb-Fe equilibrium
diagram (ref. 11) and can vary in iron content from 58 to 78 at.% (46 to 67 wt.%).
[b]Very strong.
[c]Strong.
[d]Very very weak.
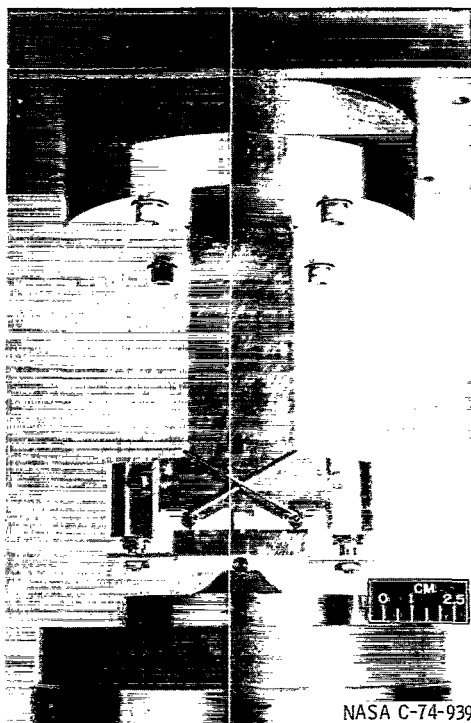
(a) Room temperature test arrangement.   (b) Liquid nitrogen bath test arrangement.
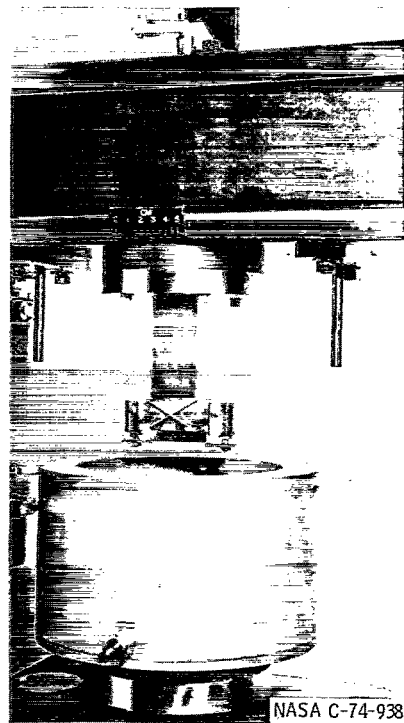
Figure 1. - Slow bend apparatus for determining fracture toughness.
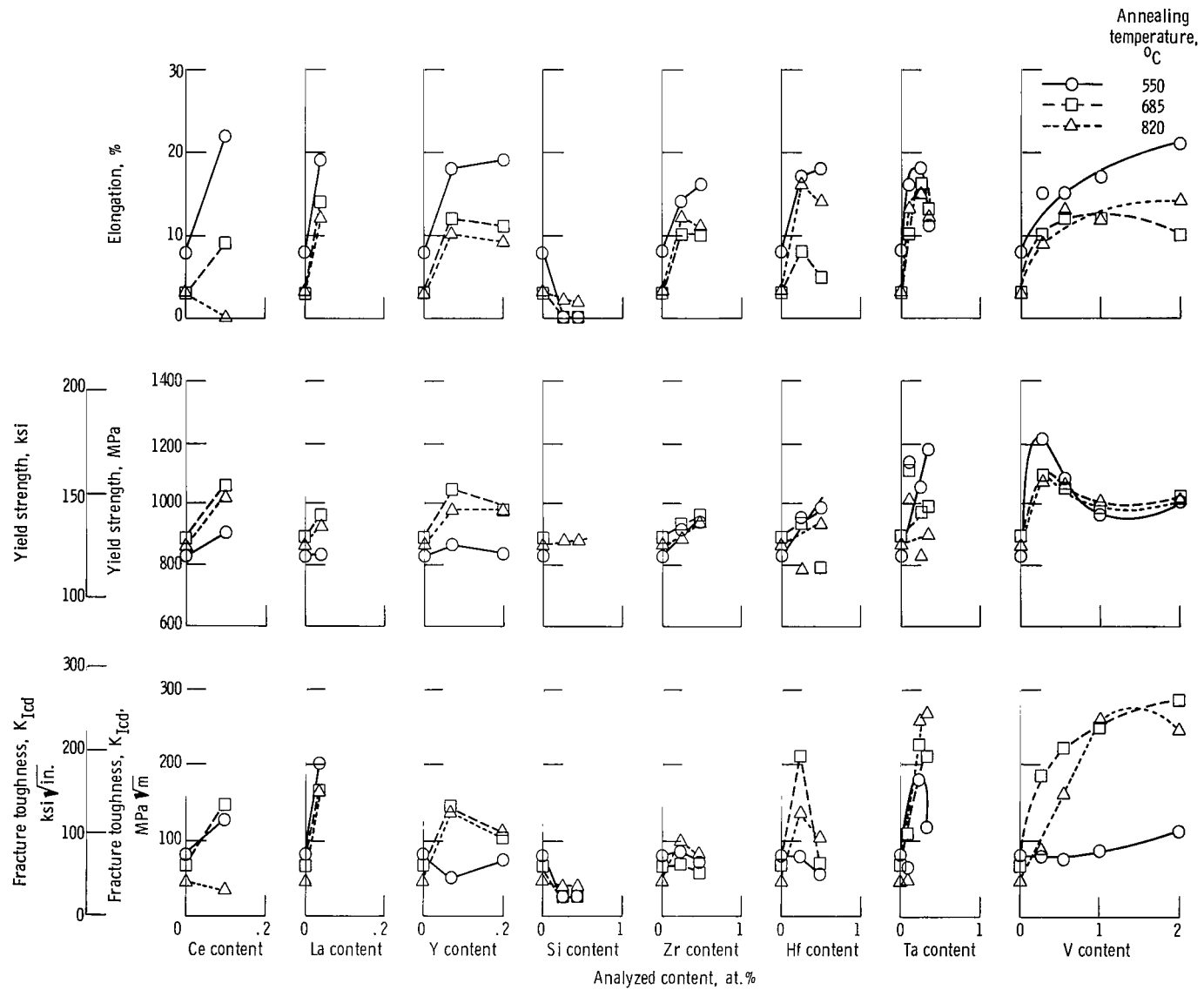
Figure 2. – Fracture toughness, yield strength, and total elongation of Fe-12Ni alloys at -196^0 C as function of reactive metal concentration for three annealing temperatures.
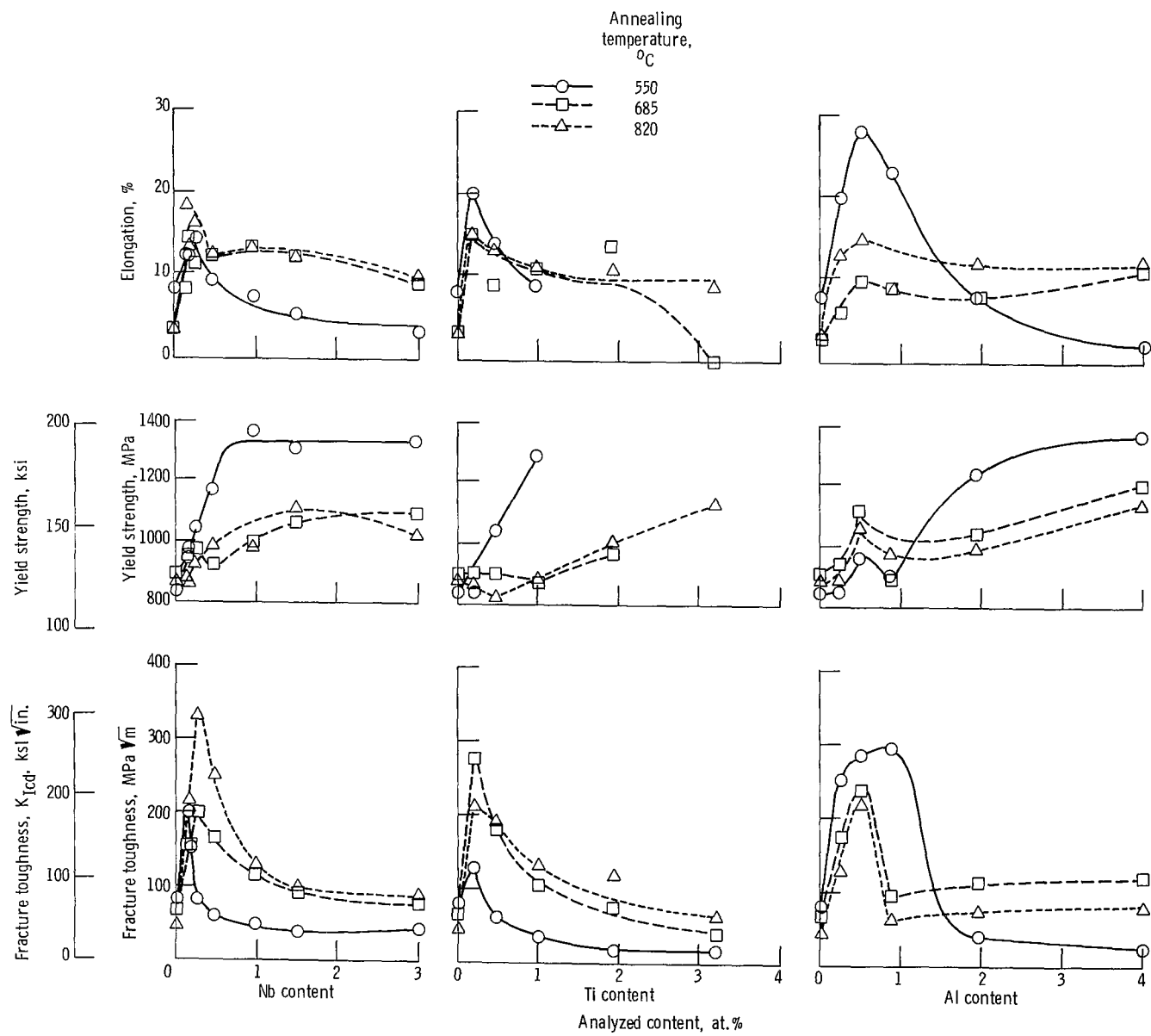
Figure 2. - Concluded.
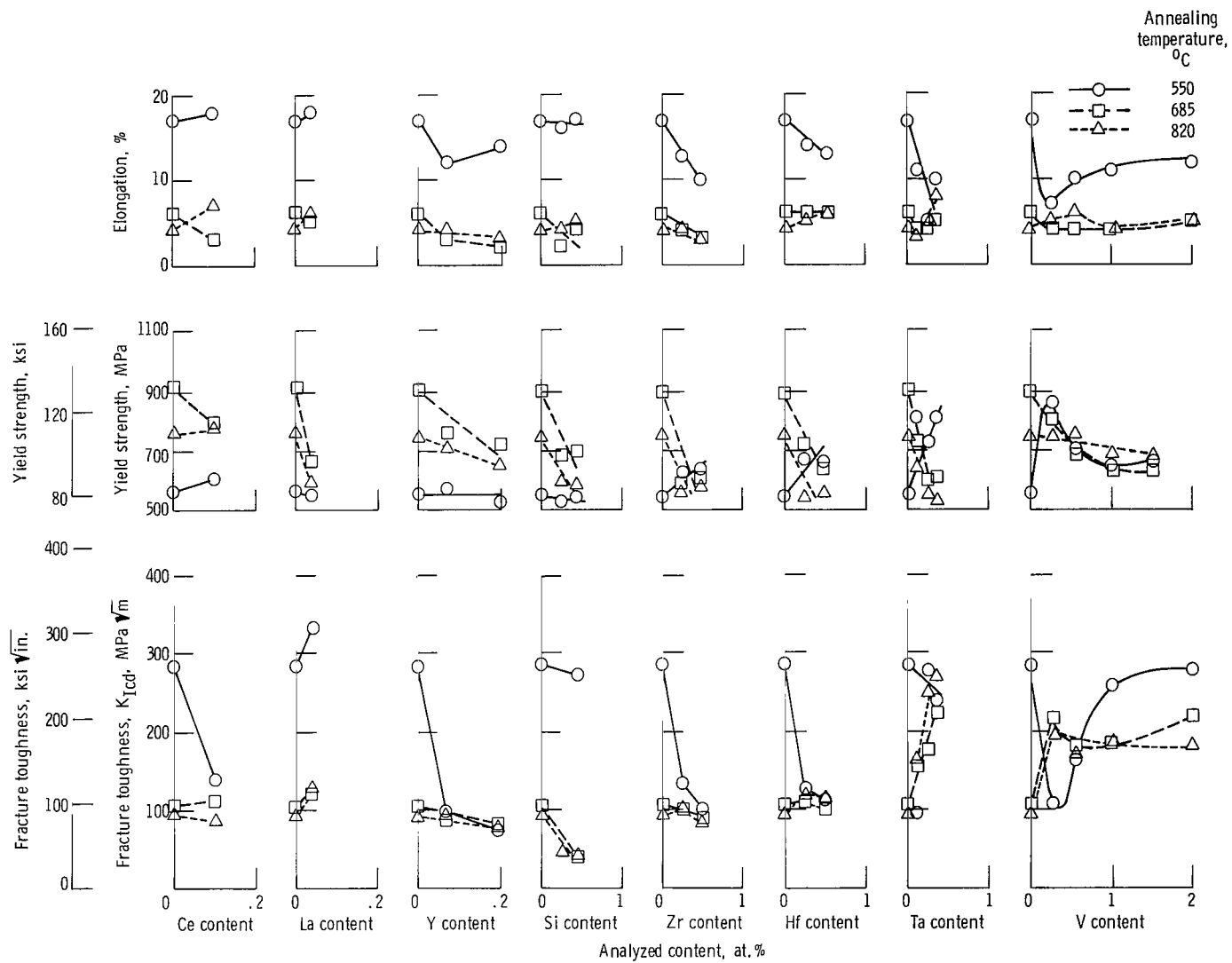
Figure 3. – Fracture toughness, yield strength, and total elongation of Fe–12Ni alloys at 25^0 C as function of reactive metal concentration for three annealing temperatures.

Figure 3. – Concluded.
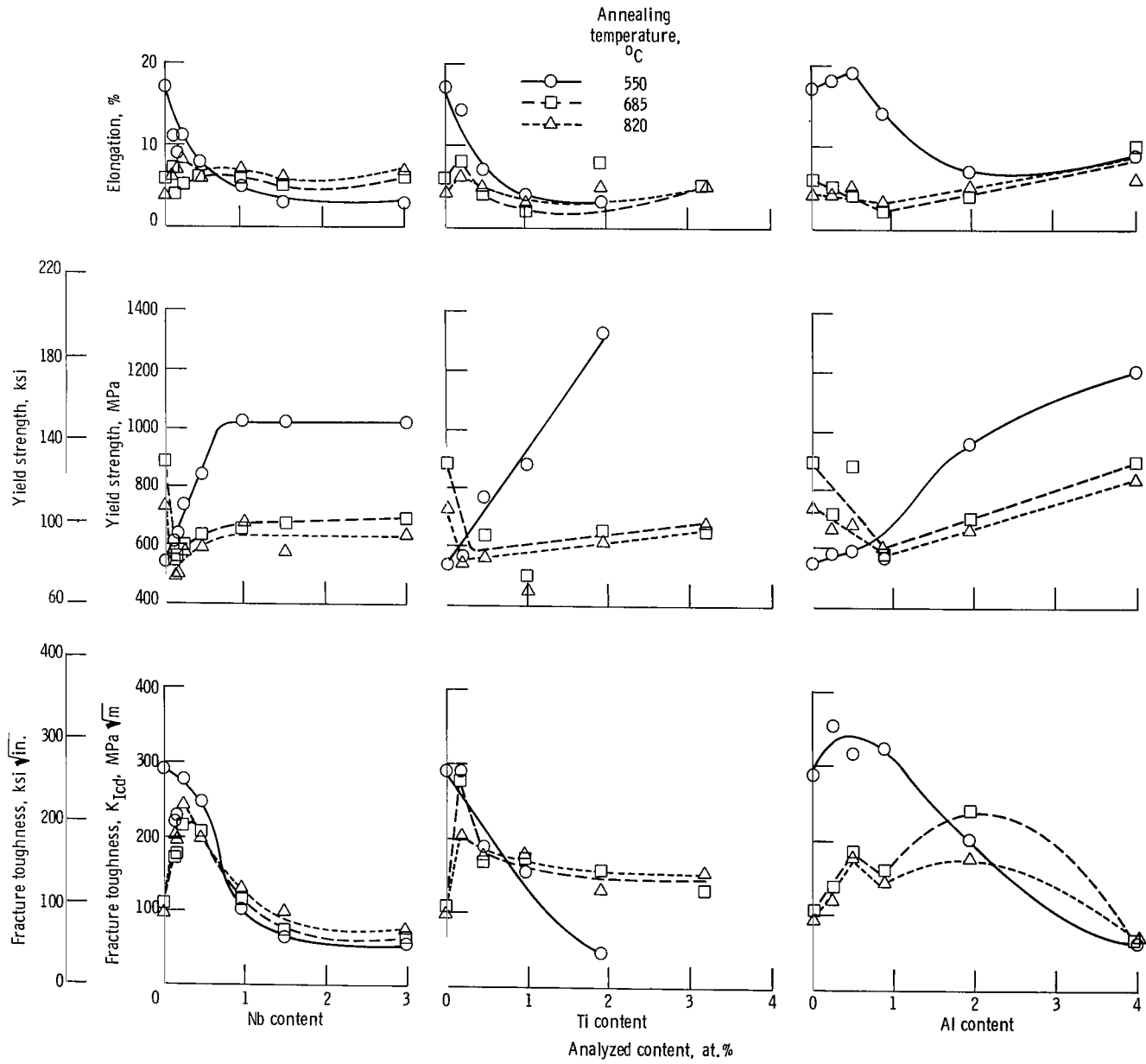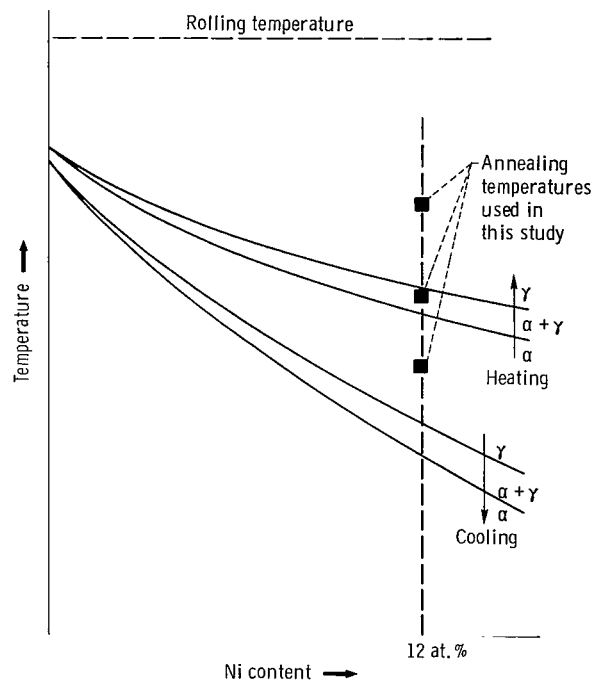
Figure 4. – Phase transformation diagram for Fe-Ni alloys on continuous heating and cooling (ref. 9).

(a) Annealing temperature, 550° C.
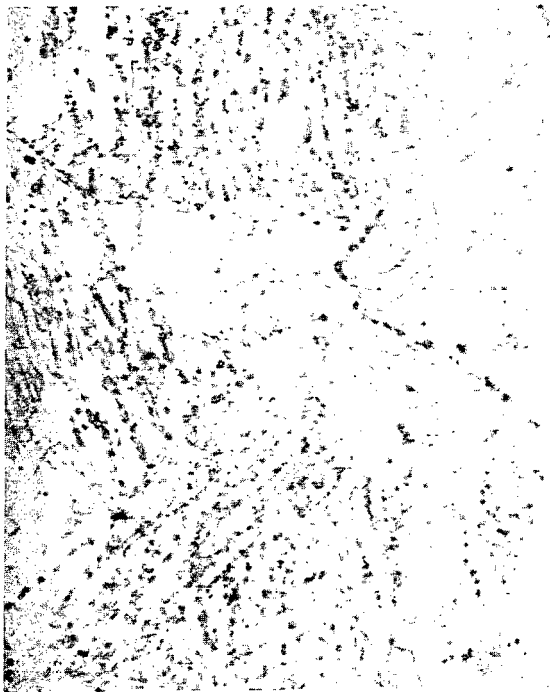
(b) Annealing temperature, 685° C.
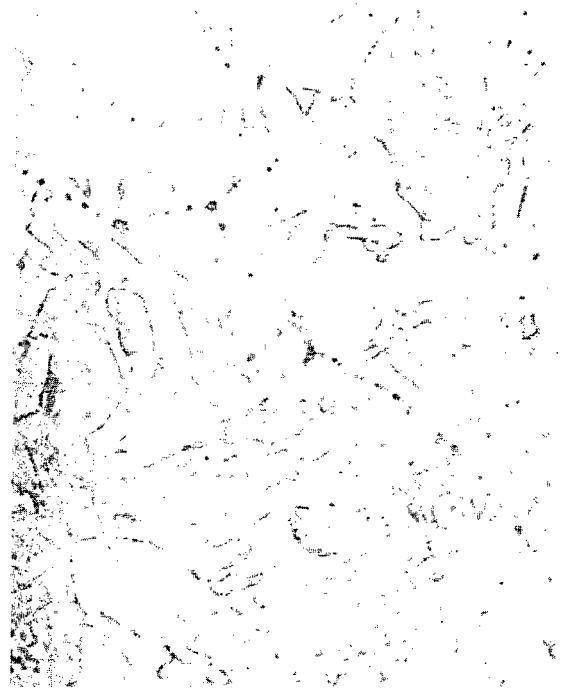
(c) Annealing temperature, 820° C.

Figure 5. - Microstructure of Fe-12Ni binary alloy. X1000.
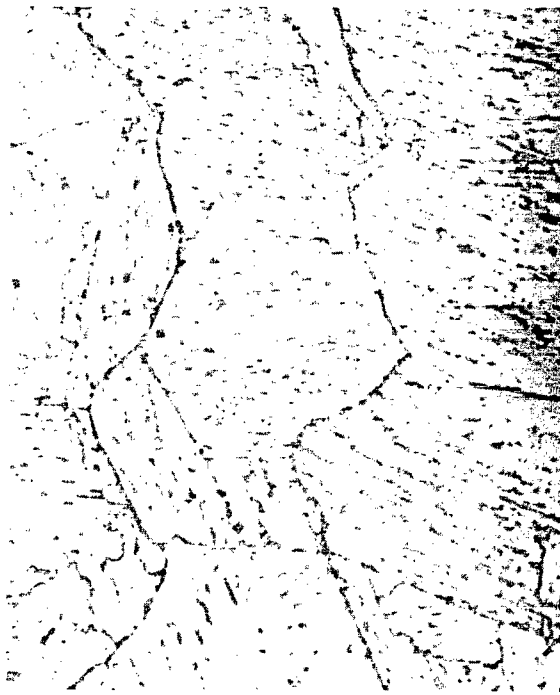
(a) Annealing temperature, 550° C.

(b) Annealing temperature, 685° C.

(c) Annealing temperature, 820° C.

Figure 6. - Microstructure of Fe-12Ni-0.5Al alloy. X1000.

29

(a) Annealing temperature, 550° C.
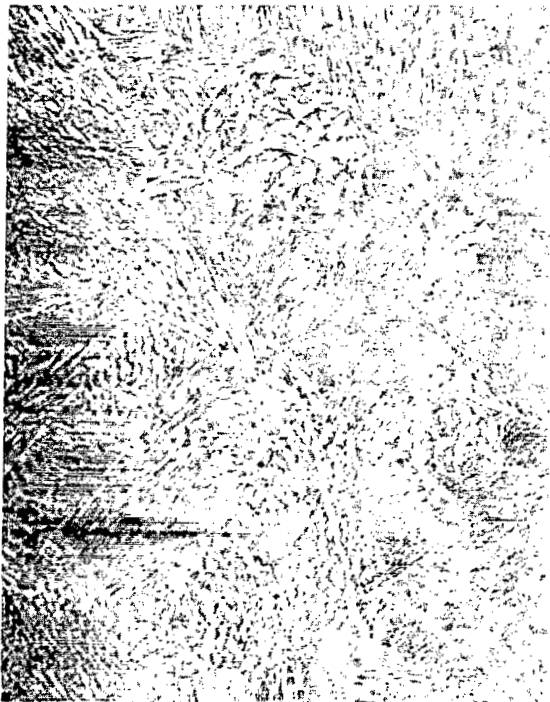
(b) Annealing temperature, 685° C.
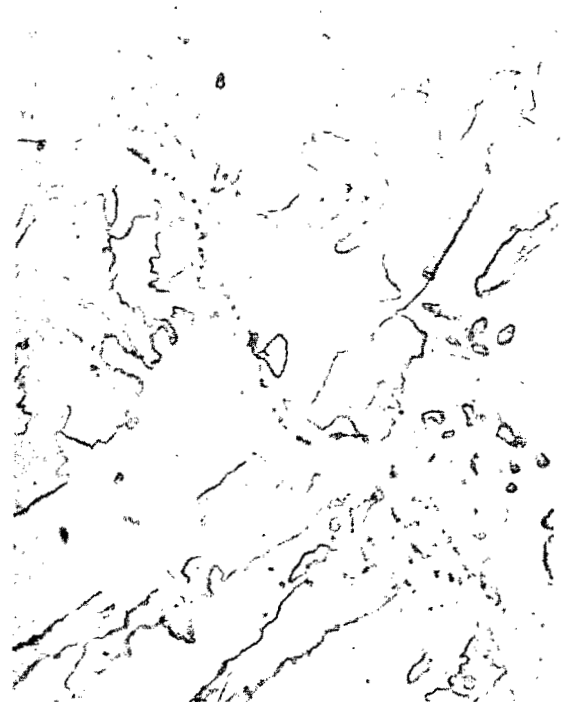
(c) Annealing temperature, 820° C.

Figure 7. - Microstructure of Fe-12Ni-0.25Nb alloy. X1000.

30

(a) Fe-12Ni. Annealed at 550°C; fracture toughness, K_{Icd} (-196°C) = 80 MPa $\sqrt{m}$ (73 ksi $\sqrt{in.}$).

(b) Fe-12Ni-0.5Al. Annealed at 550°C; fracture toughness, K_{Icd} (-196°C) = 284 MPa $\sqrt{m}$ (258 ksi $\sqrt{in.}$).

(c) Fe-12Ni-0.25Nb. Annealed at 550°C; fracture toughness, K_{Icd} (-196°C) = 80 MPa $\sqrt{m}$ (73 ksi $\sqrt{in.}$).

(d) Fe-12Ni-0.25Nb. Annealed at 820°C; fracture toughness, K_{Icd} (-196°C) = 329 MPa $\sqrt{m}$ (299 ksi $\sqrt{in.}$).

Figure 8. - Transmission electronmicrographs of selected Fe-12Ni base alloys.

31
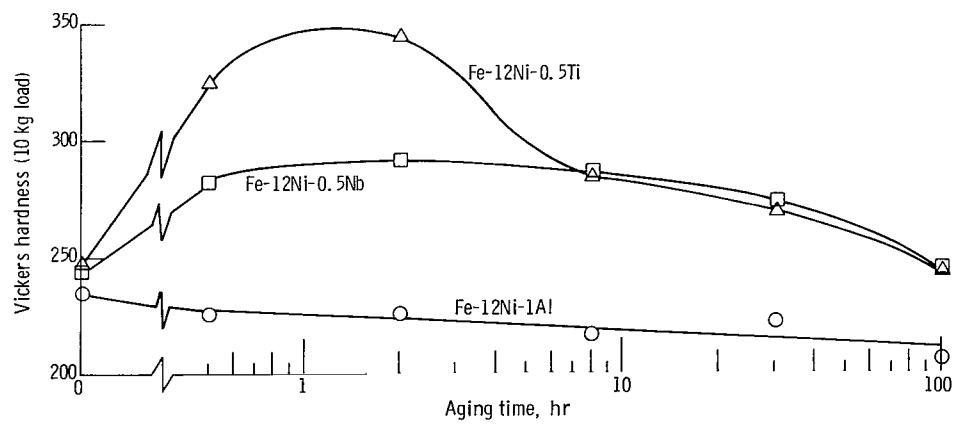
Figure 9. - Effect of aging time at 550⁰ C on hardness of hot-rolled Fe-12Ni alloys.
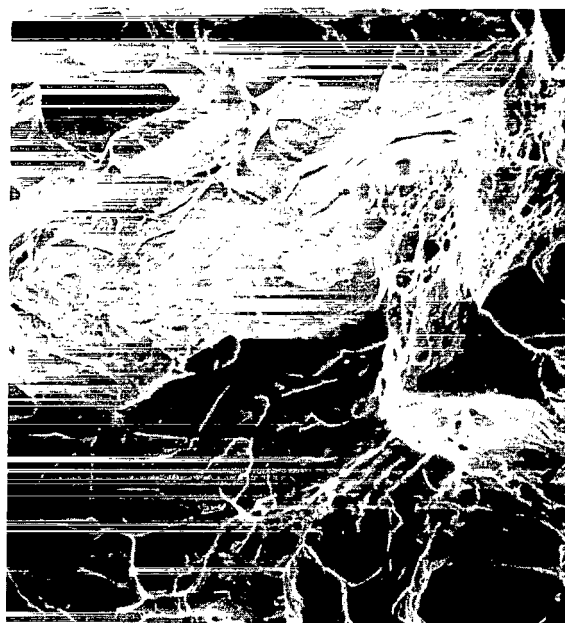
(a) Annealing temperature, 550° C.
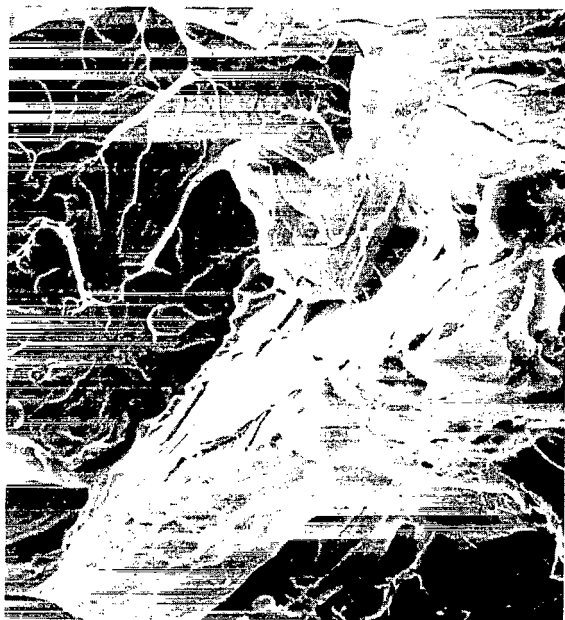
(b) Annealing temperature, 685° C.

(c) Annealing temperature, 820° C.

Figure 10. - Fractographs of fracture toughness specimens of Fe-12Ni-0.25Nb tested at -196° C. X500.
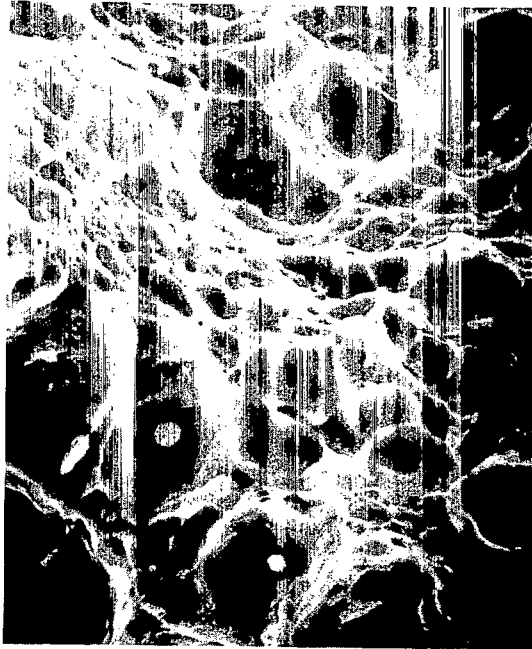
(a) Annealing temperature, 550° C.
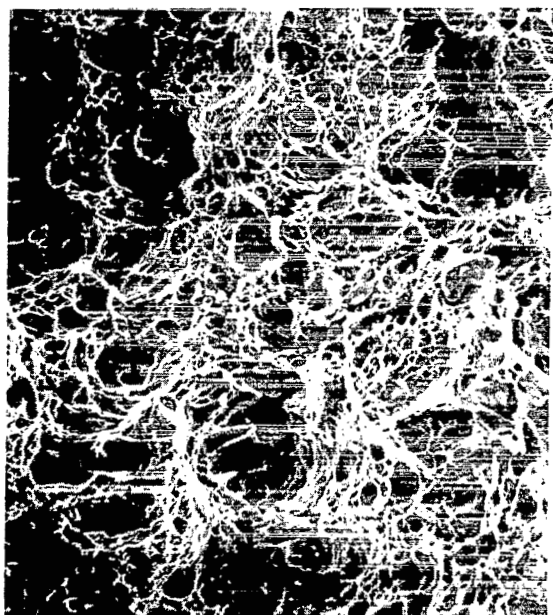
(b) Annealing temperature, 685° C.
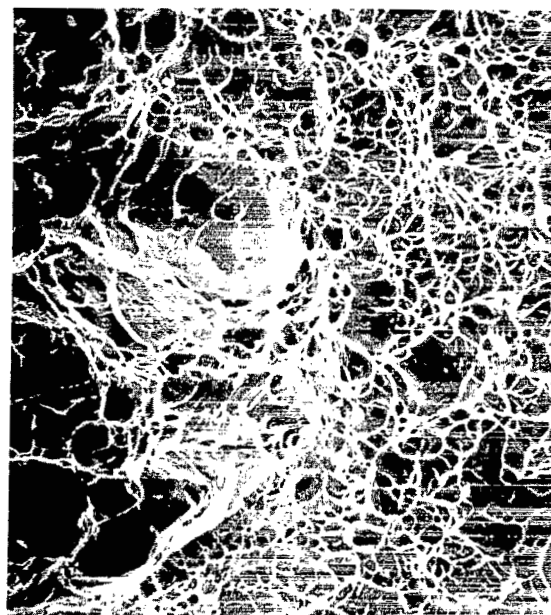
(c) Annealing temperature, 820° C.

Figure 11. - Fractographs of fracture toughness specimens of Fe-12Ni-0.5Al tested at -196° C. X500.

Figure 12. - Fractograph of fracture toughness specimen of Fe-12Ni-0.25Hf annealed at 820° and tested at -196° C. X2500.

(a) Test temperature, -196° C.

(b) Test temperature, 25° C.
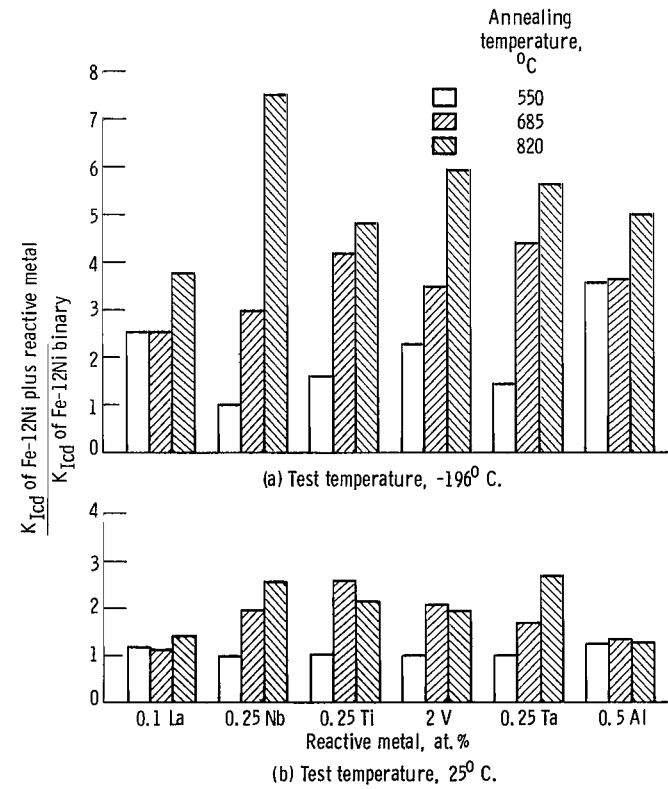
Figure 13. - Comparison of fracture toughness improvements in Fe-12Ni resulting from nominal reactive metal additions.
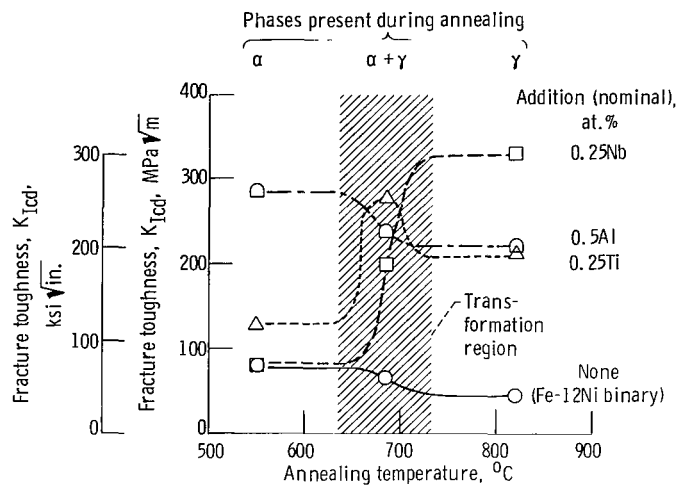
Figure 14. – Variations in toughness response at -196° C due to annealing near or within α→γ transformation region as shown by various reactive metal additions to Fe-12Ni at their optimum concentrations (2-hr anneals).
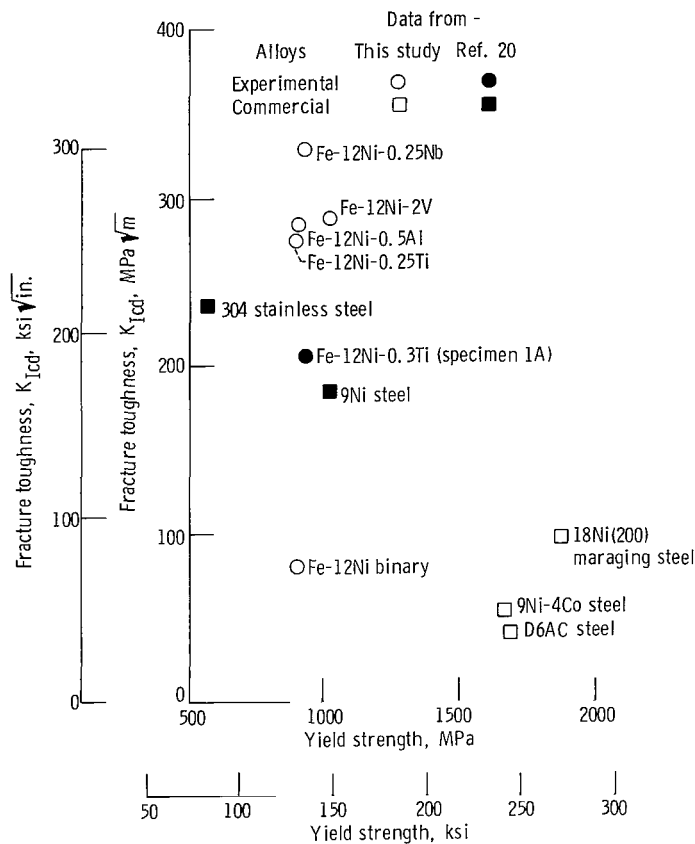

Figure 15. – Comparison of toughness/yield strength values of Fe-12Ni alloys with various commercial steels tested at -196° C. All fracture toughness values from slow bend tests on precracked Charpy specimens evaluated by equivalent energy method.

36

"The aeronautical and space activities of the United States shall be
conducted so as to contribute . . . to the expansion of human knowl-
edge of phenomena in the atmosphere and space. The Administration
shall provide for the widest practicable and appropriate dissemination
of information concerning its activities and the results thereof."
—NATIONAL AERONAUTICS AND SPACE ACT OF 1958

NASA SCIENTIFIC AND TECHNICAL PUBLICATIONS

TECHNICAL REPORTS: Scientific and
technical information considered important,
complete, and a lasting contribution to existing
knowledge.

TECHNICAL NOTES: Information less broad
in scope but nevertheless of importance as a
contribution to existing knowledge.

TECHNICAL MEMORANDUMS:
Information receiving limited distribution
because of preliminary data, security classifica-
tion, or other reasons. Also includes conference
proceedings with either limited or unlimited
distribution.

CONTRACTOR REPORTS: Scientific and
technical information generated under a NASA
contract or grant and considered an important
contribution to existing knowledge.

TECHNICAL TRANSLATIONS: Information
published in a foreign language considered
to merit NASA distribution in English.

SPECIAL PUBLICATIONS: Information
derived from or of value to NASA activities.
Publications include final reports of major
projects, monographs, data compilations,
handbooks, sourcebooks, and special
bibliographies.

TECHNOLOGY UTILIZATION
PUBLICATIONS: Information on technology
used by NASA that may be of particular
interest in commercial and other non-aerospace
applications. Publications include Tech Briefs,
Technology Utilization Reports and
Technology Surveys.

Details on the availability of these publications may be obtained from:

SCIENTIFIC AND TECHNICAL INFORMATION OFFICE

NATIONAL AERONAUTICS AND SPACE ADMINISTRATION

Washington, D.C. 20546